UNIVERSITÀ DEGLI STUDI DI MESSINA

Dipartimento di Medicina Clinica e Sperimentale

Dottorato di Ricerca in Scienze Biomediche Cliniche e Sperimentali

XXXIV Ciclo

Coordinatore: Ch.mo Prof. Francesco Squadrito

DWI BOWEL RATIOS: NEW INDEXES FOR CROHN'S DISEASE ACTIVITY AT MAGNETIC RESONANCE ENTEROGRAPHY?

Tesi di Dottorato:

Dott. Giuseppe **Cicero**

SSD: Med36

Relatore:

Ch.mo Prof. Silvio **Mazziotti**

Anno accademico 2020-2021

INDEX

INTRODUCTION

Crohn's disease (CD) is an intestinal chronic inflammatory condition characterized by periodic periods of recurrence and remission [1].

It is mainly spread in in North America and Western Europe with a peak age of onset in the 2nd–4th decades of life [1, 2].

To date, the precise etiology of Crohn's disease (CD) remains not completely understood, since its occurrence derives from the combination of genetic, immunologic, environmental risk factors [2].

This results in a transmural inflammation of the intestinal walls that can arise anywhere within the gut, from the mouth to the anus [2].

However, it usually affects both the terminal ileum and colon (approximately 50% of the patients), with smaller percentages of isolated small-bowel (30%) or colonic (20%) involvement [1, 2].

Final diagnosis of CD is achieved through the combination of clinical picture, laboratory tests and endoscopy with biopsy.

Nevertheless, imaging plays a pivotal role for the intestinal assessment of CD patients and all the radiological modalities can be employed each characterized by pros and cons.

Fluoroscopic techniques, such as barium follow-through, historically represented the first radiologic modality able in displaying peristaltic alterations, strictures and mucosal abnormalities. However, the radiation exposure and the advent of cross-sectional imaging, with their detailed appraisal of bowel wall and extraintestinal structures, led fluoroscopy falling out of favor [3].

Conversely, ultrasound (US) takes advantage from the wide availability, low healthcare costs and lack of ionizing radiation.

Its efficacy has been widely demonstrated in CD and some additional and emerging techniques, such as color-Doppler, Small Intestine Contrast-Enhanced Ultrasonography (SICUS), contrast-enhanced US (CEUS) and Elastosonography, may further improve the evaluation of intestinal

loops. Nonetheless, US is highly operator-dependent, which can result in low inter-observer reproducibility [4, 5].

Computed Tomography with enterographic protocol (CTE) provides a comprehensive assessment of the whole abdominal cavity, allowing the detection of intestinal CD lesions as well as extra-enteric complications.

Moreover, the fast scan times make this technique performable also on claustrophobic patients.

However, the well-known limit of CTE consists in the radiation exposure which may vary on the basis of the number of enhanced phases acquired and usually ranging from 6 to 28 mSv [2, 5].

This represents a significant concern in CD patients, who are often young and usually need frequent follow-up examinations [5].

Finally, Magnetic Resonance Enterography (MRE) overcomes the drawbacks of CTE, providing an exhaustive appraisal of the abdominal cavity and its content without any radiation delivery.

Its importance for bowel assessment has been largely established and it is currently considered the preferred imaging modality in CD patients, unless general contraindications to MRI are present [2, 5, 6].

An optimal fluid dilation of small bowel loops is crucial for a correct assessment of small bowel loops at MRE, since lack of distention can lead to misinterpretation of the intestinal findings.

This is achieved through the intake of an enteric contrast agent obtainable by oral assumption (MR-Enterography) or administration through a nasojejunal tube [7, 8].

The latter technique takes the name of "MR-Enteroclysis" and can provide some advantage in distension of ileojejunal loops [2, 5, 7].

However, oral drinking is generally better tolerated by the patient due to the lack of invasive maneuvers [2, 8].

Moreover, radiation exposure in case of fluoroscopic positioning of the tube is another weakness of MR-Enteroclysis [7].

A low-residue diet (4-5 days) and fasting (4-6 h) before the exam are generally recommended.

These precautions decrease the intraluminal residue and debris within small as well as large bowel, allowing a faster and more homogenous intestinal filling [9].

In the adult population, an assumption of 1–2 L of enteric contrast agent solution over 30-50 minutes is suggested in order to uniformly distend the intestinal loops and avoid intestinal absorption of the water component [2, 9].

Three main categories of contrast enteral agents can be employed for intestinal distention [5]. Gadolinium (Gd) chelates, manganese ions, ferrous ions and blueberry juice are named as "positive", due to their hyperintensity on T1-weighted scans, which however may impair detection of mural hyperenhancement after intravenous Gadolinium injection. Therefore, their use is not generally recommended [5].

Negative contrast agents determines low signal intensity on T2-weighted and include superparamagnetic iron oxides (SPIOs) solutions. However, the main drawback consists in the low palatability and the possibility of susceptibility effects.

On the other hand, for MRE performance, general consensus has been reached on the routinely use of biphasic contrast media, which appear hypointense on T1-weighted images and hyperintense on T2-weighted images thus improving the contrast between the bowel lumen and mural signal intensity [5].

The biphasic enteral agents include polyethylene glycol, barium sulfate and methylcellulose water solutions [5, 7, 10].

In order to decrease misinterpretation caused by artifacts related to peristalsis, such as intraluminal flow voids or spasm, intravenous spasmolytic agents such as hyoscine butylbromide (10 mg) or glucagon (0.2-1 mg) can be injected before the exam starts [2, 5, 7, 10].

The scanning protocol is composed of different types of sequences.

Half-Fourier Acquisition Single-shot Turbo spin Echo (HASTE) scans are usually obtained with and without fat-saturation and provide an optimal appraisal of intestinal opacification, wall thickenings and mural alterations of the intensity signal [5, 7-10].

True fast imaging with steady-state precession (True- FISP) or balanced fast field-echo (B-FFE) images take benefits from the low sensitivity to the peristaltic movements, avoiding flow-void artifacts, and from the high contrast resolution among the bowel walls, the lumen and mesenteric fat tissue. However, they can be impaired by susceptibility and black boundary artifacts at the fat-water interface [5, 7, 9, 10].

Coronal and/or axial diffusion-weighted sequences (DWI) are also obtained at a b-values ranging from 0 to 800/1000 sec/mm^2 [7]. Mural hyperintensity has been variously related to intestinal CD involvement [5].

2D or 3D spoiled T1-weighted fat-saturated ultrafast gradient-echo sequences are then acquired at baseline and after Gadolinium injection (0.2 mg/Kg at a rate of 2-3 mL/sec), usually at 30 sec (arterial phase), 70 sec (enterographic phase") and 90 sec to 7 min (delayed phase) [5, 7, 9, 10].

Additional sequences, such as T2-weighted RARE "fluoroscopic" images, Cine true FISP sequences and T1-weighted scans without fat-saturation can be also obtained in order to provide further characterization of intestinal involvement [5, 9-11].

On the basis of the clinical course and the imaging findings, four patterns of CD can be recognized: active inflammatory, penetrating/fistulizing, fibrotic/stenotizing and reparative-regenerative [1].

The active inflammatory one is characterized by transmural inflammation with wall thickening (>3 mm), presence of superficial and deep ulcers and granulomas [5].

Intestinal hyperemia, due to dilation of vasa recta (the so-called "comb-sign"), perivisceral mesenteric changes, such as edema and fat proliferation, and lymphadenopathies typically coexist [5].

At MRE, active inflammation is usually detected as mural hyperintensity on T2-w scans, restricted diffusion on DWI images at the highest b-value and hyperenhancement in the arterial phase that progressively increases throughout all the following phases [2, 5, 10].

The penetrating pattern is caused by the development of intramural ulcers into mesenteric sinus tracts, fistulas and abscesses [2, 12].

These pathologic structures are usually better visualized on DWI scans and after Gd injection.

While the formers appear as hyperintense and hyperenhanced linear tracks, perhaps communicating with other loops, hollow organs or the skin surface, the latter is detected as an air/fluid collection with avidly enhancing peripheral walls [2, 10, 12].

The mesenteric distortion may cause adhesions with consequent intestinal obstruction [5].

The fibrostenotic subtype of CD is characterized by wall thickening with narrowing of the bowel lumen, causing local stricture and dilation of the upstream intestinal loops.

This is generally caused by a longstanding disease with fibrotic involution.

Chronic fibrotic strictures are generally hypointense on both T1- and T2-weighted sequences, with none or slight hyperintensity on DWI scans and progressive enhancement with a peak appreciable in the delayed phase [5, 10, 12].

T2-weighted, Cine and fluoroscopy-MR images can be helpful in highlighting the stricture [2, 5, 10].

The reparative and regenerative type represent, at least from the radiological point of view, a quiescent stage of the disease.

This subtype is characterized by mucosal atrophy with superimposition of reparative polyps.

Restricted diffusion, hyperenhancement, engorgement of vasa recta and lymphadenopathies are not identifiable [10, 12].

On the basis of the supramentioned radiological and MRE findings, several attempts have been made over the years for assessing and monitoring CD activity through comparison with clinical and endoscopic features.

However, endoscopy implies an invasive procedure at risk, although rarely, of complications and therefore cannot be so frequently performed.

The current indexes are described in detail in the following chapter.

ACTIVITY SCORE INDICES FOR CROHN'S DISEASE AT MRE

- **The MaRIA score and derivatives**

The Magnetic Resonance Index of Activity (MaRIA) was the first score arisen with the aim of establishing an index activity of CD using MRE [13].

MRE findings evaluated for calculating MaRIA score are: wall thickness, post-contrast wall signal intensity, relative contrast enhancement (RCE) and the presence of edema, ulcers, pseudopolyps, and lymph node enlargement [13-15].

Relative contrast enhancement (RCE) is calculated as:

[(WSI postgadolinium – WSI pregadolinium)/(WSI pregadolinium)] x 100 x (SD noise pregadolinium / SD noise postgadolinium),

where WSI is wall signal intensity [15].

The MaRIA score was then produced using a regression model based on these imaging features generated: 1.5 × bowel wall thickness in mm + 0.02 × RCE + 5 × edema + 10 × ulceration [16].

Cut-off points for active and severe disease are respectively 7 and 11 [15].

The MaRIA score has demonstrated strong correlation with endoscopic scores (CDEIS and SES-CD), moderate concordance with the Harvey Bradshaw Index (HBI) and c-reactive protein (CRP) [16, 17].

It also accurately predicts treatment response in CD patients.

Main drawbacks of MaRIA consist in time-consumption in calculating the score and lack of information about lesion length and DWI [14].

In order overcome some of these limits, the same research group had later proposed a simplified version of MaRIA score by Kim et al. in 2017 (sempliflied MaRIA or MaRIAs) [18]. MaRIAs takes into consideration only three radiological findings already included in the MaRIA score (mural thickening, mural edema and mucosal ulcerations) and adds fat stranding as a new item [14, 17, 19].

DWI findings were classified on the basis of a three-scale grade: 0, no increased diffusion restriction; 1, DWI hypersignal slightly lower than that of lymph nodes; 2, DWI hypersignal same as or higher than that of lymph nodes).

The final formula for MaRIAs is:

([1.5 × wall thickness in millimeters] + [0.02 × relative contrast enhancement] + [5 × edema] + [5 × DWI grade]) [18, 19].

In comparison to the original MaRIA score, the authors demonstrated a similar correlation to CDEIS and did not differ in the ability to diagnose active or severe inflammation [17].

Moreover, interobserver-agreement has been found excellent with a significant decrease of calculation time (from 17.14 min of the original MaRIA to 4.77 min recorded for MaRIAs) [14, 19].

However, authors included as a limit of their work a visual and thus subjective estimation of DWI findings with possible consequent inter-observer variability [18].

- **The Clermont score**

The Clermont score firstly introduced the variables of DWI and ADC values for small-bowel assessment in CD in patient in 2013 [20].

Patients included in the study did not receive any bowel cleansing or rectal preparation and the MaRIA score was used as reference standard [20].

The estimation of disease activity on Clermont score relies on the evaluation of four variables: wall thickening, ulcers, edema, and ADC values [20].

The calculation of Clermont score was derived using a multivariate linear regression model: −1.321 × ADC (mm2/s) + 1.646 × wall thickening + 8.306 × ulcers + 5.613 × edema + 5.039 [20].

In detecting active disease, hyperintensity on DWI scans showed high sensitivity (100%), specificity (92.9%), predictive negative value (94.4%) and predictive positive value (100%) [20].

ADC inversely correlated with MaRIA score and calculation of ROC curve showed a threshold of 1.6 mm^2/s for distinction of active from non-active CD [20].

A strong correlation of the Clermont score with MaRIA score has also been found for ileal CD but not for colonic CD localization [21].

A Clermont score >8.4 was found to be predictive of active ileal disease and a score $\geq$ 12.5 of severe ileal disease [17, 20, 21].

- **CDMI and MEGS**

Another score for assessing activity of intestinal CD has been proposed by Steward et al., and it is also known as "London score", "Crohn disease MRI index" (CDMI) or "Crohn's Disease Activity Score" (CDAS).

The authors performed MRE on CD patients before undergoing surgical operation and MRI scans on the surgical specimens.

The reference standard used was the acute inflammation score (AIS), a histopathological grading system that assess mucosal ulcerations, edema quantity and depth of neutrophilic infiltration [22].

The parameters evaluated for CDMI were: mural thickness, mural T2 signal, perivisceralT2 signal, mural enhancement pattern, degree of enhancement, lymph nodes and lymph nodes enhancement. However, since only the former two demonstrated correlation in a univariable, multivariable and backward selection, the final formula for calculating CDMI was constructed as follows:

CDMI = 1.79 + 1.34 × mural thickness + 0.94 × mural T2 score [22].

The cut-off for CD disease activity was found to be 4.1, with a sensitivity of 0.81 and a specificity of 0.70 [22].

Makanyanga et al. in 2014 reviewed the CDMI score introducing the magnetic resonance enterography global score (MEGS) [23].

A 4-scale rate was assigned to: mural thickness (0: < 3mm; 1: 3-5 mm; 2> 5-7 mm; 3: > 7 mm); mural T2 signal (0: equivalent to normal bowel wall; 1: minor increase; 2: moderate increase; 3: marked increase); peri-mural T2 signal (0: equivalent to normal mesentery; 1: increase in

mesenteric signal without fluid; 2: fluid rim < 2mm; 3: fluid rim > 2 mm); T1 enhancement (0: equivalent to normal bowel wall; minor enhancement; 2: moderate enhancement; 3: marked enhancement); haustral loss (0: none; 1: <1/3 segment; 2: 1/3 to 2/3 segment; 3: >2/3 segment). Mural enhancement pattern was scored as: 0 if not appreciable or homogenous, 1 if mucosal, 2 if layered.

5 points are added if lymph nodes ≥1 cm (short axis diameter), comb sign, fistulae or abscesses are present.

The length of CD lesions was used to provide a multiplication factor for each individual segmental score: 0–5 cm×1; 5–15 cm×1.5; >15 cm×2

The sum of the supramentioned indexes per each segment (jejunum, ileum, terminal ileum, cecum, ascending, transverse, descending, sigmoid and rectum based) results in the final MEGS score.

Correlation of MEGS with both calprotectin and C-reactive protein demonstrated to be strong and higher than CDMI.

However, no significant correlation was found between MEGS and the clinical Harvey-Bradshaw score [23].

Nevertheless, MEGS also showed to well relate to clinical responders to treatment with TNF-α than non-responders [24].

- **The Nancy score**

The Nancy score was born with the intention of assessing activity index on inflammatory bowel disease (IBD) patients, either CD or UC.

This score is evaluated within five intestinal segments (rectum, sigmoid region, left colon, transverse colon, right colon) for UC and six for CD (ileum is also included).

At each localization, the Nancy score assesses six variables: ulceration, parietal oedema, bowel wall thickening, differentiation between mucosal-submucosal layers from muscularis propria, rapid contrast enhancement and DWI hyperintensity.

Presence of one among these radiological findings rates as a singular point (absence accounts for 0) and the final score is calculated as the sum of the numerical values obtained per each intestinal segment.

Maximum value for UC and CD are respectively 30 and 36.

Active inflammation is established by achieving a rating of >1 for UC and >2 for CD.

Results among CD patients have been strongly correlated to both SES-CD and CDEIS scores. However, the Nancy score demonstrated better accuracy for the detection of endoscopic inflammation in UC rather than CD [25].

Moreover, the Nancy score has demonstrated accurate results in predicting mucosal healing and need of surgical intervention [14, 25, 26].

ENDOSCOPIC INDICES OF CROHN'S DISEASE ACTIVITY

- **The CDEIS score**

The CD Endoscopic Index of Severity (CDEIS) was developed in 1989 by the Groupe D'etudes Therapeutiques Des Affections Inflammatoires Du Tube Digestif (GETAID) in order to estimate activity of CD and response to treatment [27, 28].

Presence of mucosal superficial and/or deep ulcers, the extent of surface involved by disease and that of the ulcerated surface, the presence of ulcerated or nonulcerated stenosis were recorded in five segments: rectum, sigmoid and left colon, transverse colon, right colon, and ileum [28, 29].

On the basis of statistical correlation results, the final formula for calculating CDEIS is:

CDEIS = 12 x ISRCF (deep ulcerations) +6xISRCF (superficial ulcerations) + ASSD (Average surface involved by the disease) + ASSU (Average surface involved by ulcerations only) +3 x PRES (non ulcerated stenosis) +3 x PRES (ulcerated stenosis).

The CDEIS score range from 0 to 44, with a direct correlation with disease severity.

Sipponen et al. found a strong correlation between CDEIS score for ileocolonic CD, fecal granulocyte proteins calprotectin and lactoferrin.

In particular, lactoferrin significantly with CDEIS for only ileal CD [29].

On the basis of this correlation, a CDEIS score below 3 suggests inactive disease, 3–9 mildly active, 9–12 moderately active and 12 severely active disease [29].

CDEIS showed high correlation with lesion severity and low inter-observer variability, which results in high reproducibility [27].

On the other hand, its use in clinical practice remains complicated as it is time-consuming and unwieldy.

In fact, it requires the evaluation of several endoscopic lesions and a strong expertise in assessing the extent of diseased mucosal surfaces and differentiating superficial from deep ulcers [27, 30].

- **The SES-CD score**

In 2004, the Simple Endoscopic Score for CD (SES-CD) has been proposed for simplifying endoscopic assessment of CD patients rather than CDEIS [31].

The endoscopic evaluation is focused on a 3-scale (0 to 3) evaluation of 4 items: ulcers, proportion of the surface covered by ulcers, proportion of the surface with any other lesions and stenosis [31].

Ulcers are scored according to their size (0.1-0.5 cm; 0.5-2 cm; >2cm), ulceration and proportion of the affected surface depending on the extent, stenosis as single or multiple and on the basis of possibility of being passed by the endoscope [31].

The final score is obtained from the sum of all the descriptors in each segment (terminal ileum, ascending colon, transverse colon, descending and sigmoid colon, rectum) and ranges between 0 and 56 [27].

SES-CD can be calculated as the sum of all variables – 1.4 x (number of affected segments) [32].

The SES-CD correlates well with the CDEIS and, compared to this one, has demonstrated better intraclass agreement between observers and higher correlation with CDAI. [27, 31]

Limitations of the SES-CD rely on the lack of cut-off values for estimating treatment response and mucosal healing [27].

Although both SES-CD and CDEIS moderately correlate with CD histological index, a better correlation has been found for SES-CD, especially at the level of terminal ileum.

On the basis of the simplicity and the better correlation with histopathology, SES-CD is currently the preferred used index [30].

- **Rutgeerts Postoperative Endoscopic Index**

Recurrence of CD can arise in 50% of patients within 3 year after surgical intervention and early endoscopic signs can be detectable at 6–12 months in up to 60–70% of patients [32].

The Rutgeerts Postoperative Endoscopic Index has been introduced in 1984 and up to now it is the only score for evaluation of CD patient who underwent surgery [27, 33].

It consists of a five grade scale: no lesions in the distal ileum (i0); <5 apthous lesions (i1); > 5 apthous lesions with normal mucosa between the lesions, or skip areas of larger lesions or lesions confined to ileocolonic anastomosis (i2); diffuse apthous ileitis with diffusely inflamed mucosa (i3); diffuse inflammation with already larger ulcers, nodules, and/or narrowing (i4) [32, 33].
Scores of 3 and 4 are validated cut-offs for predicting clinical relapse.
Afterwards, since it arose the suspicion that post-surgical ischemic lesions could lead to an overestimation of disease progression, a modification within the second class of Rutgeerts score was proposed: i2a, lesions confined to the anastomosis ≤5 isolated aphthous ulcers in the ileum; i2b, more than 5 aphthous ulcers in the ileum with normal mucosa in between, anastomotic lesions [34]. However, no differences were observed in terms of recurrence and need for surgery in these two categories [34].

AIM OF THE STUDY

DWI exploits the randomized Brownian motion of water molecules included in a particular tissue. Increase in cellular density results in reduction of water molecules movements due to the presence of cell membranes.

The impaired motion can be visually recognized as augmented intensity signal on the DWI scan itself or can be quantitatively assessed using the apparent diffusion coefficient (ADC) map, in which regions of interest (ROIs) can be drawn in order to obtain a numerical measurement [35, 36].

DWI is already included in the standard MRE protocol and its role is well-established in detection of intestinal CD lesions, since the intramural inflammatory infiltration is characterized by hyperintensity on DWI and relative low ADC values [37-40].

Several efforts have been made in order to take full advantage from its diagnostic potential which could lead to a replacement of contrast-enhanced sequences.

Over the years, DWI and ADC have been variously related to intestinal lesions in CD patients, with different cut-off values proposed for distinction of the diverse grades of active inflammation and/or fibrosis [21, 38- 43].

On one hand, the recognition of bowel wall alterations is intuitive and quite easy on DWI images, although its detection and estimation of degree rely on the subjective evaluation of the reader.

On the other hand, the quantitative valuation on the relative ADC map can be impaired by volume artifacts within the ROI, especially if the wall thickening is minimal or moderate, and the final results are not non-standardizable due to the dissimilar environmental conditions (even using the same scanner) and differences among vendors.

The aim of this work is to combine the visual assessment of DWI images at high b-values on bowel lesions in CD patient with a quantifiable parameter that could make this qualitative evaluation somehow objective.

In this context, it has been decided to compare DWI values measured on the bowel lesion with those of the mesenteric lymph nodes, the spleen and the psoas muscle through calculation of mathematical ratios.

This is the very first time that a DWI ratio is calculated in the intestinal district, since few attempts have been previously described for preoperative grading and treatment guidance in brain gliomas and in the identification of tumor recurrence following liver transplantation [44, 45].

In order to determine the clinical significance of these ratios, a correlation has been carried out with the endoscopic features assessed through SES-CD score, assumed as the standard reference.

As reported in the specific chapter, the existing MRE indices of CD are time-consuming processes, somewhat complicated and therefore poorly performed.

DWI bowel ratios with endoscopic correlation could provide a simple and rapid esteem of the disease activity that might reveal to be of great importance in the daily clinical practice.

MATERIAL AND METHODS

- **Study population**

This single-center retrospective study evaluated 59 patients with CD who underwent MRE at our institution between September 2018 and July 2021.

The inclusion criteria consisted of adult age (≥18 years old), proven diagnosis of CD, based on endoscopy with deep mucosal biopsy or histologic analysis of the bowel resection specimen and the performance of both MRE and ileocolonoscopy at an interval not greater than 4 weeks between the two.

The study was approved by local ethics committee and conducted in accordance with the latest version of Helsinki Declaration.

- **Study procedure**

  - **Endoscopic evaluation**

Ileocolonoscopic evaluation was performed using an Olympus 180 endoscopy device.

All colonic segments and the terminal ileum were satisfactorily visualized and evaluated.

In patients naïve to surgery, the severity of CD inflammation in each segment was scored according to SES-CD and CD was classified as: inactive (0–2), mild (3–6), moderate (7–15), severe (>15).

On the other hand, Rutgeerts score was used for endoscopic assessment of operated patients.

Disease activity was divided as follows: post-surgery remission (i0-i1); substantial post-surgery recurrence (i2); advanced post-surgery recurrence (i3-i4).

- **MRE protocol**

A standardized MRE protocol was performed on a 1.5T MR scanner (Achieva, Philips, Best, The Netherlands), with gradients of 33 mT/m/s and a 16-channel phased array coil placed to cover the abdomen.

All patients were asked to fast for at least 6 h before begin of the exam.

MRE was performed after assumption of a water solution of a biphasic oral contrast agent (Polyethylene glycol, 800–1500 mL), carried out 30–45 min prior the examination.

The standard MRE protocol included the following: coronal and axial half-Fourier acquisition single-shot turbo-spin echo (HASTE; TR/TE: ∞/80 ms) without fat-suppression (FS); axial and coronal true-fast imaging with steady-state (True-Fisp; TR/TE: 4.20/2.10 ms, FA: 60°); axial diffusion-weighted imaging (DWI) sequences with a diffusion b factor fixed at 0, 400 and 800 s/mm2 ; ultrafast 3D T1-weighted gradient echo fat-suppressed, obtained before and after the intravenous injection of Gadoterate Meglumine (Dotarem) at a dose of 0.2 mL/kg body-weight on axial/coronal plane, followed by a bolus of 30 mL of normal saline.

- **DWI assessment**

The MRE protocol was evaluated in consensus by two readers with different years of experience (17 and 7) in MRE imaging. All the pathologic segments were identified within the ileum.

On DWI scans, three region of interest (ROIs) were placed within the pathologic bowel wall and an average result was obtained. If multiple intestinal lesions were present, the one with the brighter intensity signal was selected. The readers visually compared DWI scans to ADC map in order to confirm water molecules restriction (Fig.1).

The same measurement approach was accomplished within mesenteric lymph nodes (when multiple, the largest one was chosen), the spleen and the psoas muscle.

When multiple lymph nodes were present, the one with the brighter signal was chosen; if similar, the largest in size.

ROIs within the spleen were preferably drawn in the subcortical region.

For positioning of ROIs, the readers were free to zoom the images (Fig 2).

Three final ratios were obtained dividing the values sampled at the level of small bowel wall with the ones of the extra-enteric structures:

1) Bowel/Lymph node Ratio (BL-ratio) = bowel DWI/lymph node DWI
2) Bowel/Spleen Ratio (BS-ratio) = bowel DWI/spleen DWI
3) Bowel/Psoas Ratio (BP-ratio) = bowel DWI/psoas DWI

- **Statistical analysis**

The categorical variables (naïve/surgery patients, SES-CD and Rutgeerts classes) were expressed as absolute frequencies and percentages. The numerical data (ileum, spleen and lymph nodes DWI, as well as the relative ratios) were expressed as mean and standard deviations score (SDS), minimum and maximum value.

Considering the small sample size, the non-parametric approach was used.

After calculations of the different ratios, the Spearman test was applied in order to assess the existence of any significant correlation among the ratios, separately for the naïve and the surgery groups of patients.

Mann–Whitney test was also applied with reference to all numerical parameters to evaluate any statistically significant differences between two patient groups (naive vs surgery patients).

In order to visualize the trend of the ratios mean values within the different Rutgeerts and SES-CD classes, box plot graphs have been realized.

The Jonckheere- Terpstra (J-T) test has been used in order to verify the existence of a monotonic increase of the ratios within the different SES-CD and Rutgeerts classes.

With reference to the resulting significance of J-T test, box-plot graphs have been created for each ratio in order to display the distribution within the SES-CD classes (remission, mild, moderate and severe activity) only for the naïve patients group.

A p-value smaller than 0.05 was considered statistically significant.

Statistical analysis was performed using IBM SPSS Statistics for Windows, Version 20 (Armonk, NY, IBM Corp.) [46, 47].

Fig.1 Identification and selection of the pathologic ileal segment

Coronal Haste T2- weighted (a), axial DWI at b-800 s/mm^2 (b) and the relative ADC map (c). The

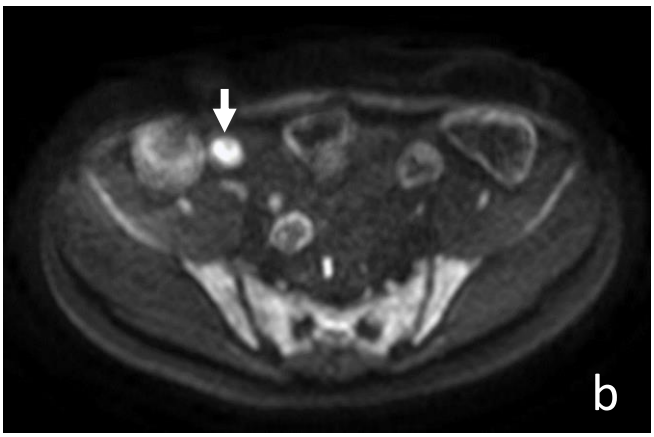

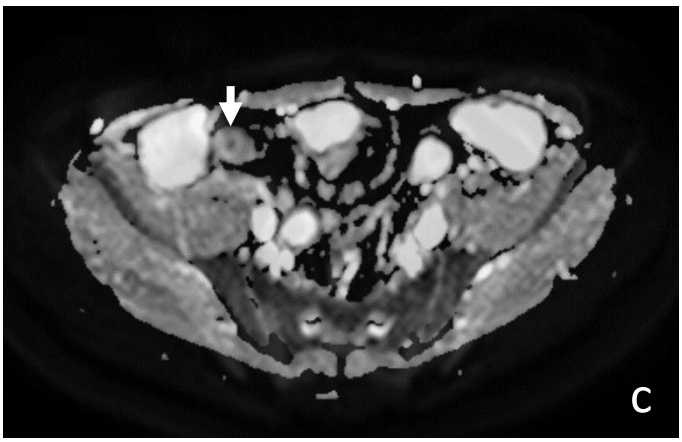

evaluation of the full protocol aided the identification and selection of the pathologic loop (arrow) which is characterized by wall thickening on Haste T2-weighted scans, hyperintensity on DWI images and drop of signal intensity on ADC map.

Fig.2 Measurements on DWI scans

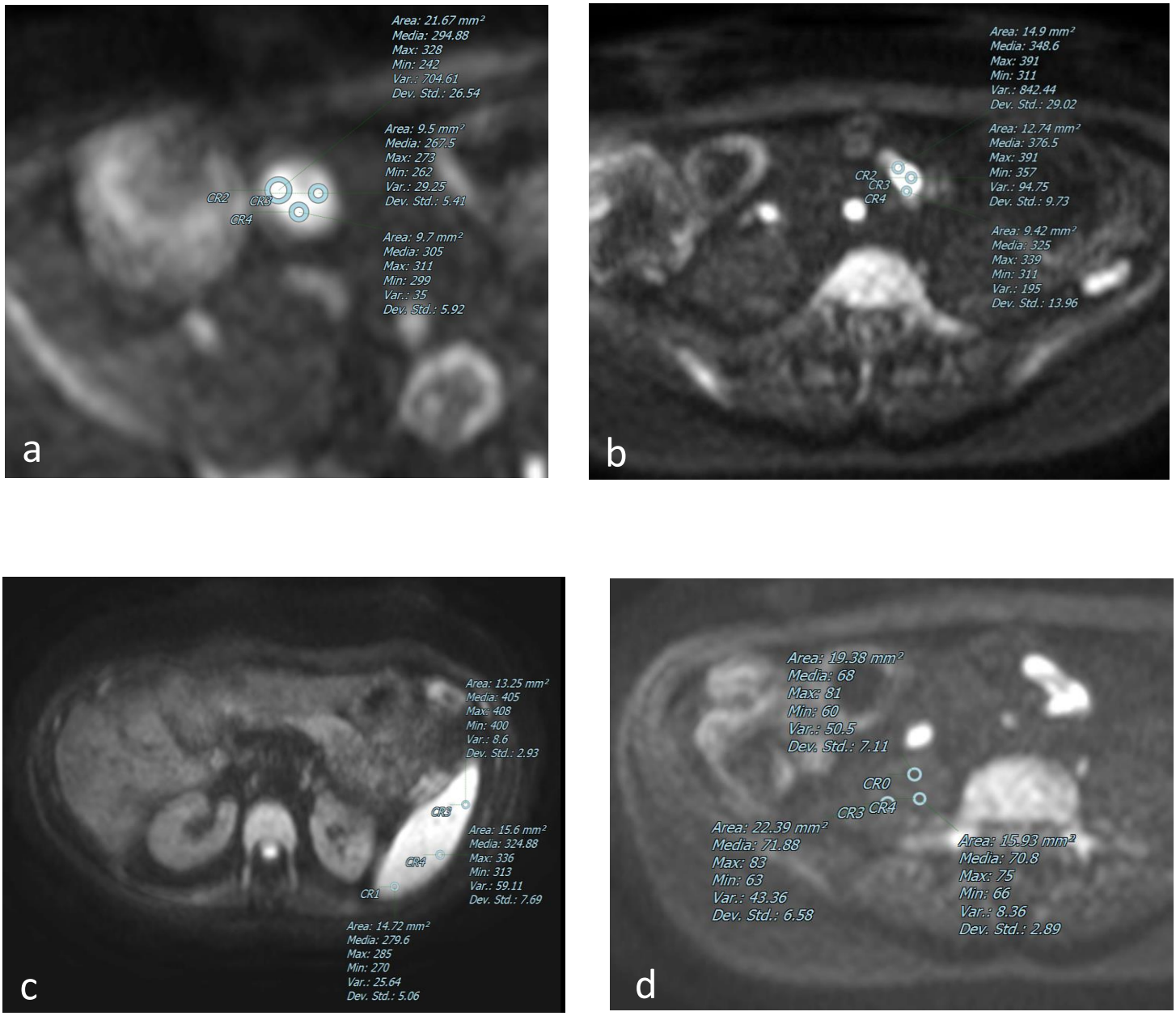

1. Example of ROI positioning on Axial DWI images within the bowel walls (a), the lymph nodes (b), the spleen (c) and the psoas muscle (d) on the same patient of Fig.1. Three ROI were located within each structure and an average value was obtained. The readers were free to zoom the images in order to avoid partial volume artifacts.

RESULTS

Age of the patients ranged between 18 to 79 years old, with a mean age of 44.

Male patients were prevalent within the study cohort (35; 60%).

39 patients (66%) were naive to surgery, while 20 patients (34%) had intestinal resection.

Naïve-to-surgery patients were distributed within the different SES-CD score classes as follows: inactive (19; 48,7%); mild activity (10; 25,6%); moderate activity (7; 17,9%); severe activity (3; 7,7%).

Surgery patients were distributed within the different Rutgeerts score classes as follows: post-surgery remission (1; 5%), substantial post-surgery recurrence (4; 20%); advanced post-surgery recurrence (15, 75%).

Descriptive statistics about numerical variables in total and for each group (naïve and surgery patients) are summarized in Table 1 to 3.

Tab.1 ***Descriptive statistics for all the patients***

	n	**mean**	**standard deviation**	**minimum value**	**maximum value**
Bowel DWI	46	289.4	161.8	92	1128
Spleen DWI	37	321.0	179.8	108.6	918
BS ratio	37	1.0	0.6	0.3	2.5
Psoas DWI	46	71.5	22.8	42.1	181.5
BP ratio	46	4.1	1.6	1.4	9.4
Lymphnode DWI	46	319.8	140.1	114	864.9
BL ratio	46	0.9	0.3	0.5	1.4

Tab.2 ***Descriptive statistics for non-operated patients***

	n	mean	standard deviation	minimum value	maximum value
Bowel DWI	26	284.35	197.27	96.1	1128
Spleen DWI	21	281.20	102.54	108.6	461.6
BS ratio	21	1.03	0.62	0.4	2.5
Psoas DWI	26	72.81	26.9	42.1	181.5
BP ratio	26	3.86	1.5	1.4	7.8
Lymph node DWI	26	326.07	148.61	114	864.9
BL ratio	26	0.85	0.23	0.5	1.3

Tab.3 ***Descriptive statistics for surgical patients***

	n	mean	standard deviation	minimum value	maximum value
Bowel DWI	20	295.95	103.49	92	471
Spleen DWI	16	373.28	241.69	141	918
BS ratio	16	0.96	0.46	0.3	1.8
Psoas DWI	20	69.89	16.65	46	99.9
BP ratio	20	4.33	1.68	1.8	9.4
Lymphnode DWI	20	311.55	131.57	151	671
BL ratio	20	0.98	0.26	0.6	1.4

Within the surgery patient group, the only significant positive correlation was found between the BL-ratio and BP-ratio (r_S= 0.539; p=0.014).

Within the naïve patient group a significant positive correlation has been found among SES-CD classes and the different ratios: BS (r_S= 0.464; p=0.034); BP (r_S= 0.506; p=0.008); BL (r_S= 0.495; p=0.010).

Moreover, a significant positive correlation has been found also for BL-ratio/BP-ratio (r_S= 0.387; p=0.046) and BS/BP ratio (r_S= 0.550; p=0.010).

Mean and SD of the different ratios for each SES-CD and Rutgeerts class is summarized in Table 4 and 5 and visually displayed in Graph 1 and Graph 2.

Table 4. ***Mean and SD values for each SES-CD class in non-operated patients***

		BS Ratio	BP Ratio	BL Ratio
Remission	**Mean**	0.84	2.89	0.69
	SD	0.72	0.96	0.21
Mild activity	**Mean**	1.02	3.8	0.88
	SD	0.47	1.03	0.19
Moderate activity	**Mean**	1.13	4.51	0.96
	SD	0.75	1.86	0.21
Severe activity	**Mean**	1.5	5.13	0.97
	SD	0.14	1.85	0.31
Total	**Mean**	1.04	3.87	0.85
	SD	0.62	1.51	0.23

Table 5. ***Mean and SD values for each Rutgeerts class in surgical patients***

		BS Ratio	BP Ratio	BL Ratio
Remission	**Mean**	0.3	3.9	0.6
	SD	0.0	0.0	0.0
Substantial recurrence	**Mean**	1.4	4.5	1.08
	SD	0.49	1.04	0.22
Advanced recurrence	**Mean**	0.87	4.31	0.99
	SD	0.36	1.9	0.26
Total	**Mean**	0.97	4.33	0.99
	SD	0.47	1.69	0.26

Graph 1. ***Means of the different ratios for each SES-CD class***

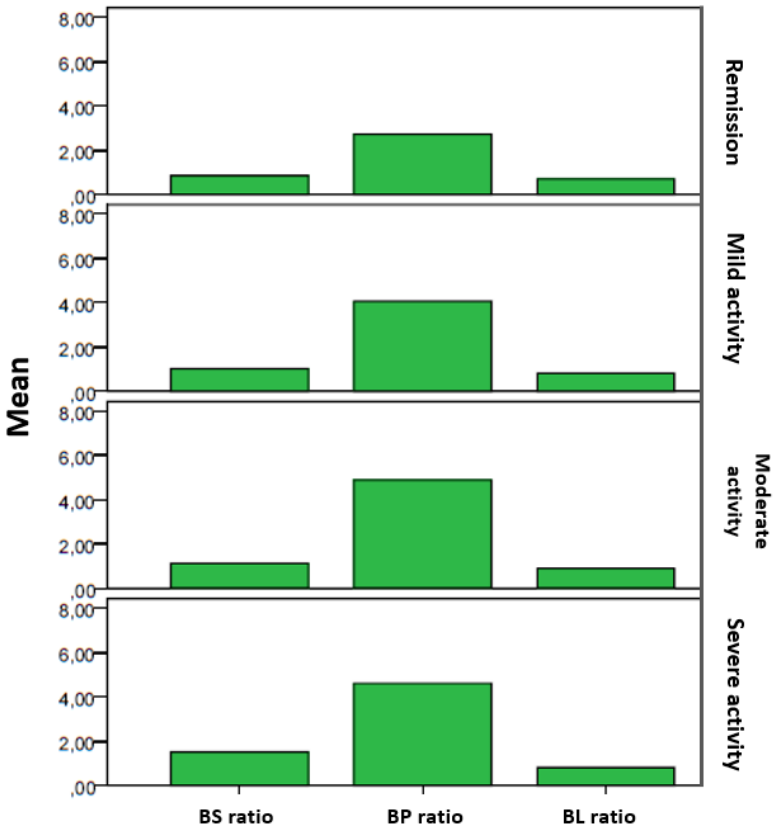

Graph 2. ***Means of the different ratios for each Rutgeerts class***

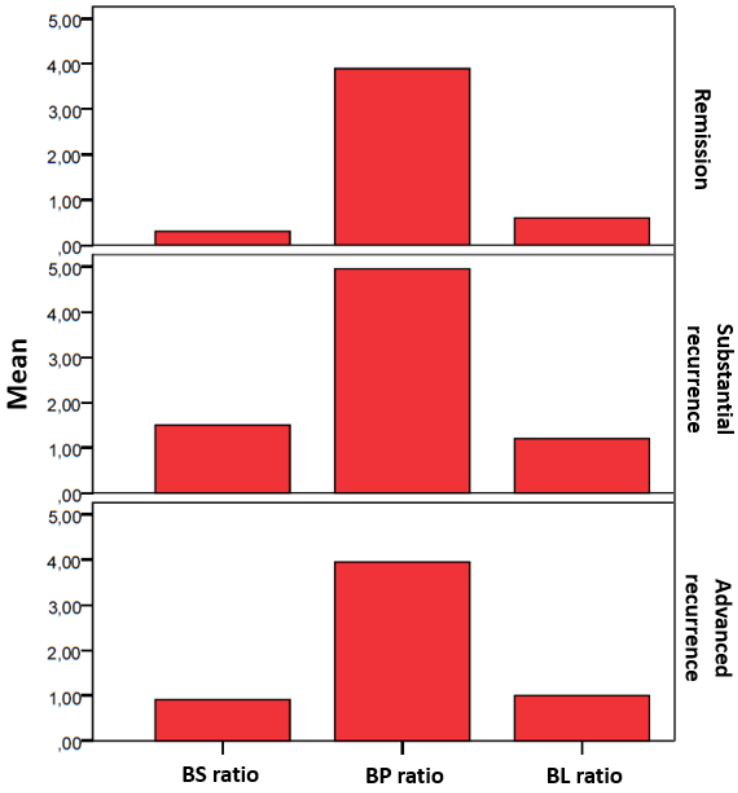

No significant statistical differences have been found between the two groups of patients for the different variables (p-value >0.050).

The J-T test has demonstrated an increasing monotonic trend for BP and BL ratios and the four SES-CD classes (Table 6; Graphs 3 to 5).

Table 6. ***J-T test for non-operated patients***

	BS Ratio	**BP Ratio**	**BL Ratio**
Number of levels	3	3	3
Numerosity	19	23	23
Observed J-T statistics	82.000	127.0	133.000
J-T mean	60.000	88.0002	88.000
J-T sd	13.252	17.714	17.455
J-T standard statistics	1.660	2.202	2.578
Asymptotic sig. 2-sided	0.097	0.28	0.010

Graph 3. ***J-T boxplot for BS ratio***

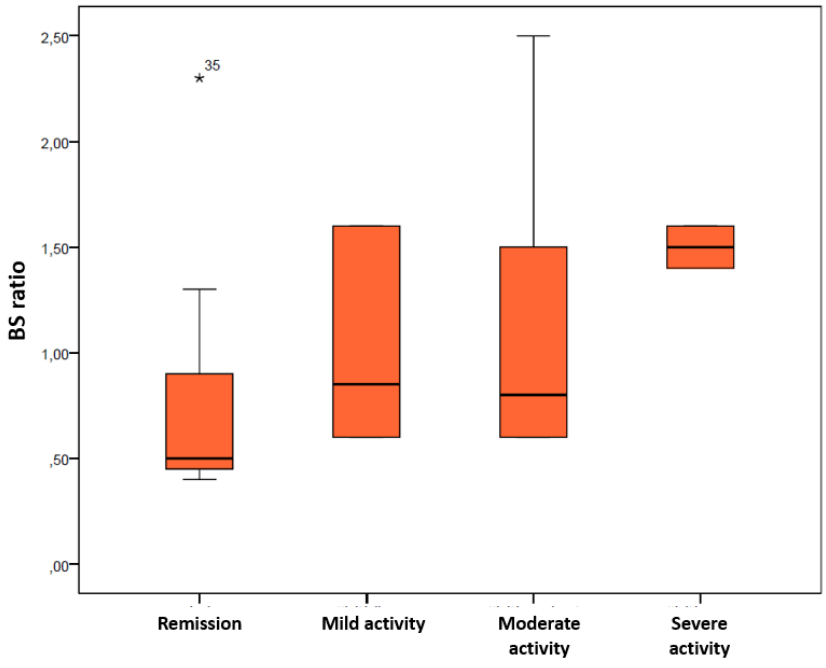

Graph 3. ***J-T boxplot for BP ratio***

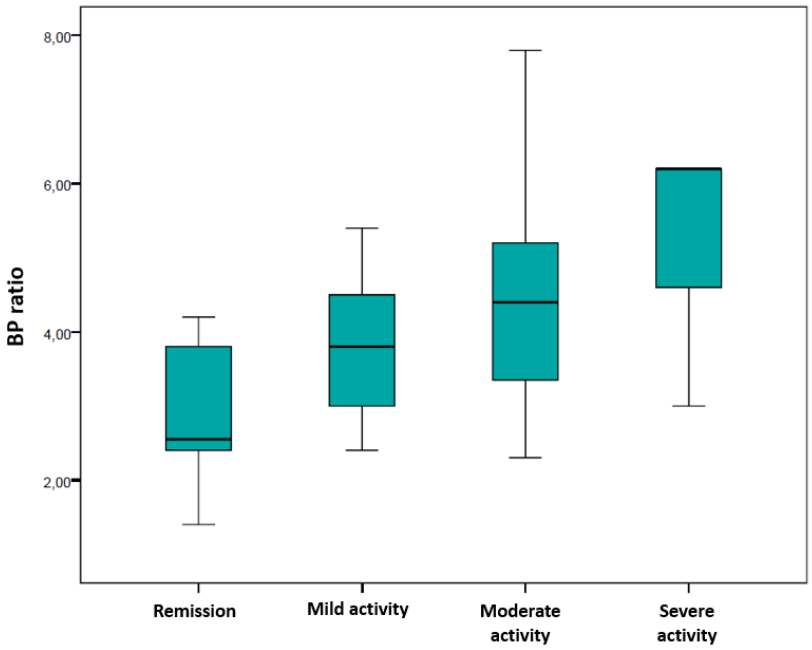

Graph 3. ***J-T boxplot for BL ratio***

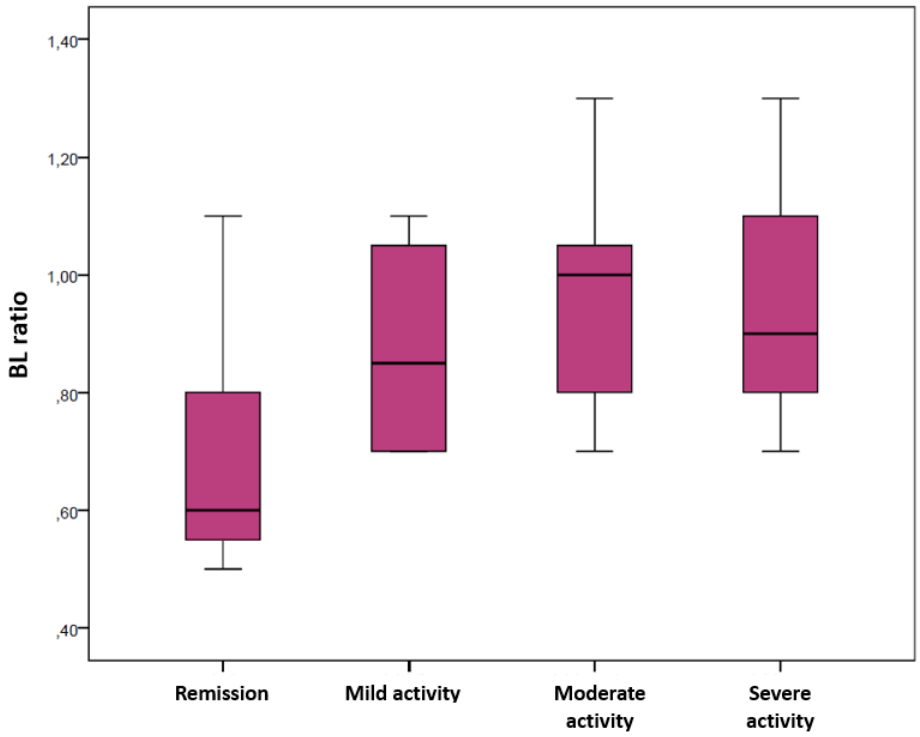

DISCUSSION

DWI imaging has been introduced in 1986 and it was first applied in neuroradiological diagnostics [48].

Its performance on the intestinal district dates back to 2009 thanks to the work of Oto et al. who firstly correlated bowel wall inflammation with an increased signal on DWI scans and lower ADC values in CD patients [40].

Since then, the diagnostic potential of DWI scans has been extensively explored and it is now routinely included in standard MRE protocols worldwide [49].

DWI images and ADC map have demonstrated the capability in distinguishing bowel segments affected by CD, both active and inactive, from normal loops [37-40].

Hyperintensity on DWI images at high b-values (>800 s/mm^2) derives from restricted diffusion of water molecules and it is confirmed by low signal intensity on the relative ADC map, which provides a quantitative parameter [21, 38-43].

This phenomenon is thought to be determined by a combination of inflammatory phenomena, such as immune cells infiltration, lymphatic ducts enlargement and granulomas formation.

Nevertheless, Freiman et al., analyzing DW-MRI data of pediatric Crohn's disease patients with the intravoxel incoherent motion model, showed that reduction of ADC values is mainly caused by fast diffusion restriction, due to microvascular alteration, rather than Brownian motion of water molecules, referable to immune infiltration [41, 50-52].

To date, a number of studies have been focused on the role of DWI and ADC in assessing inflammation and fibrosis, with consequent establishment of different thresholds for CD activity [13, 32, 52-55].

Nevertheless, addition of DWI to conventional MRE seems provide only a marginal benefit [56, 57].

However, it is important to remind that visual and quantitative assessment of DWI scan has been conducted in heterogeneous ways and relying on different reference standards.

In order to perform qualitative assessment of small bowel CD lesions, some authors made a comparison to the signal intensity of mesenteric lymph nodes, spleen, renal cortex or adjacent normal loops on DWI scans, whereas others relied on their own expertise, avoiding any landmark [53, 54, 57, 58].

Visual assessment of bowel inflammation on DWI images has been found to strictly correlate with faecal calprotectin levels and MEGS [59, 60].

On the side of quantitative assessment, several studies focused their attention on the use of ADC for activity degree distinction with related cut-off values helpful in distinguishing actively inflamed from uninflamed and in predicting disease remission [20, 21, 38, 40, 58, 61-63].

However, in CD lesions inflammation often coexists with fibrotic involution, which can act as a further confounder [58].

Moreover, low ADC values referable to fibrosis seem to correlate to histology and gain of contrast medium enhancement better than active inflammation does.

Moreover, ADC values and the use of higher b-values DWI scans (up to 3,000 sec/mm2) has demonstrated encouraging result in distinguishing inflammatory alterations from malignancies [49, 64].

However, ADC values cannot be standardized, due to technical parameters such as slice thickness, differences among vendors and environmental conditions [65-69].

This particularly applies in the intestinal field, since further variables, such as peristalsis, poor intraluminal distention, slightly thickened wall, number of the involved segments, possibility of average artifacts in ROI positioning, contribute in making ADC measurement prone to low grades of reproducibility [53, 56, 57, 59].

Therefore, radiologists generally tend to rely more on a qualitative assessments of DWI and ADC images than the quantitative ADC values [57, 70].

This work has demonstrated a statistically significant correlation between endoscopic SES-CD classes and DWI ratios measured on ileum, lymph nodes and spleen.

Moreover, the same result has been found comparing BS with BP ratios and BP with BL ratios.

These outcomes confirm, on a quantitative base, the assumption that bowel walls affected by CD can be successfully compared to lymph nodes and the spleen for the quantification of inflammation degree on DWI scans.

Up to now, this concept was only empirically expressed on the basis of a qualitative and thus subjective evaluation.

Since the evaluation of lymph nodes on DWI scans could be influenced by reactive inflammatory phenomena and that the spleen parenchyma have an inhomogeneous structure, the psoas muscle has been chosen as more “stable” point of reference.

As a matter of fact, BP ratio well correlated with BL and BS ratios.

Furthermore, a significant positive trend has been found between BP and BL ratios and the SES-CD classes.

This mean that bowel ratios can be reliably used for assessment of inflammation degree at least in patients that did not undergo surgical intervention.

On the other hand, no statistically significant correlation has been found between the DWI values or ratios and the different Rutgeerts classes, apart from that of BP and BL ratios.

This could be explained by post-surgery alterations.

Moreover, the sample size of operated patient was lower than the naïve group and further studies with larger populations may overturn this result.

Limitations of this work must be acknowledged.

First, the monocentric and retrospective evaluation and the relative small sample size.

Second, laboratory tests have not been included in the study because in the majority of the cases they were not simultaneous to the dates of MRE or colonoscopy performance. This correlation is advocated in future studies in order to further confirm or disprove the results of this work.

Finally, although the whole protocol has been examined in order to better identify the pathologic intestinal segment, the measurements have been obtained on DWI scans, which can be prone to motion or gas artifacts.

CONCLUSIONS

This work was conceived with the intent of finding a new method for the estimation of inflammatory degree in CD patients using MRE.

Over the last decade, several methods that exploit MRE findings have been proposed and are currently available for radiologists and clinicians.

However, despite their robust validation against endoscopic and clinical scores, the use of these radiologic algorithms still remains far from the daily clinical practice.

The main reason relies on their inherent complexity and time consumption in order to calculate the final score.

DWI bowel ratio seems to overcome these limitations.

Since it is based on DWI scans, the identification of the intestinal segment affected by CD as well as the lymph nodes and the spleen are intuitive and the related measurements are therefore easy to perform.

Previous studies focused their attention on the quantitative assessment of DWI scans provided by ADC map in evaluating the intestinal disease.

However, ADC values are not standardized due to their variability related to different vendors or environmental conditions.

DWI Bowel ratio do not deliver an absolute numerical value but it derives from a computation of measurements recorded on different structures.

This encourages the idea that, even using different MR scanners in various ambient conditions, the results would be similar.

The MRE outcomes achieved in this work are also corroborated by endoscopy, which is unanimously considered the gold standard for intestinal assessment in CD.

Although this is a preliminary study, Bowel DWI ratios seem to represent a consistent parameters in the radiologic evaluation of CD patients, at least in those naïve to surgery.

Obviously, considering the limits of the work, Bowel DWI ratios do not pretend to replace the already existing MRE score.

Nevertheless, it could be considered as a fast approach for achieving an indication about the possible endoscopic class in which the patient could be categorized.

Another advantage would be represented by the unnecessary administration of the intravenous contrast medium, which would avoid any risk of allergic reaction and decrease the healthcare costs.

This work could therefore pave the way to a new, fast and non-invasive method for quantification of the intestinal inflammation degree.

REFERENCES

1. Feuerstein JD, Cheifetz AS. Crohn Disease: Epidemiology, Diagnosis, and Management. Mayo Clin Proc. 2017 Jul;92(7):1088-1103. doi: 10.1016/j.mayocp.2017.04.010. Epub 2017 Jun 7. PMID: 28601423.
2. Leyendecker JR, Bloomfeld RS, DiSantis DJ, Waters GS, Mott R, Bechtold RE. MR enterography in the management of patients with Crohn disease. Radiographics. 2009 Oct;29(6):1827-46. doi: 10.1148/rg.296095510. PMID: 19959524.
3. Cicero G, Mazziotti S. Crohn's disease at radiological imaging: focus on techniques and intestinal tract. Intest Res. 2021 Oct;19(4):365-378. doi: 10.5217/ir.2020.00097. Epub 2020 Nov 25. PMID: 33232590.
4. Grand DJ, Harris A, Loftus EV Jr. Imaging for luminal disease and complications: CT enterography, MR enterography, small-bowel follow-through, and ultrasound. Gastroenterol Clin North Am. 2012 Jun;41(2):497-512. doi: 10.1016/j.gtc.2012.01.015. PMID: 22500531.
5. Masselli G, Gualdi G. MR imaging of the small bowel. Radiology. 2012 Aug;264(2):333-48. doi: 10.1148/radiol.12111658. PMID: 22821694.
6. Allen BC, Leyendecker JR. MR enterography for assessment and management of small bowel Crohn disease. Radiol Clin North Am. 2014 Jul;52(4):799-810. doi: 10.1016/j.rcl.2014.02.001. Epub 2014 Apr 1. PMID: 24889172.
7. Amzallag-Bellenger E, Oudjit A, Ruiz A, Cadiot G, Soyer PA, Hoeffel CC. Effectiveness of MR enterography for the assessment of small-bowel diseases beyond Crohn disease. Radiographics. 2012 Sep-Oct;32(5):1423-44. doi: 10.1148/rg.325115088. PMID: 22977028.
8. Costa-Silva L, Brandão AC. MR enterography for the assessment of small bowel diseases. Magn Reson Imaging Clin N Am. 2013 May;21(2):365-83. doi: 10.1016/j.mric.2013.01.005. Epub 2013 Feb 19. PMID: 23642558.

9. Sinha R, Verma R, Verma S, Rajesh A. MR enterography of Crohn disease: part 1, rationale, technique, and pitfalls. AJR Am J Roentgenol. 2011 Jul;197(1):76-9. doi: 10.2214/AJR.10.7253. PMID: 21701013.
10. Kaushal P, Somwaru AS, Charabaty A, Levy AD. MR Enterography of Inflammatory Bowel Disease with Endoscopic Correlation. Radiographics. 2017 Jan-Feb;37(1):116-131. doi: 10.1148/rg.2017160064. Epub 2016 Nov 25. PMID: 27885894.
11. Cicero G, Pallio S, D'Angelo T, Mazziotti S. Lipomatosis of the ileocecal valve: A not to miss diagnosis when performing magnetic resonance enterography. Clin Case Rep. 2021 May 24;9(5):e04316. doi: 10.1002/ccr3.4316. PMID: 34084526; PMCID: PMC8142311.
12. Sinha R, Verma R, Verma S, Rajesh A. MR enterography of Crohn disease: part 2, imaging and pathologic findings. AJR Am J Roentgenol. 2011 Jul;197(1):80-5. doi: 10.2214/AJR.11.6740. PMID: 21701014.
13. Rimola, J.; Rodriguez, S.; García-Bosch, O.; Ordas, I.; Ayala, E.; Aceituno, M.; Pellisé, M.; Ayuso, C.; Ricart, E.; Donoso, L.; et al. Magnetic resonance for assessment of disease activity and severity in ileocolonic Crohn's disease. Gut 2009, 58, 1113–1120
14. D'Amico F, Chateau T, Laurent V, Danese S, Peyrin-Biroulet L. Which MRI Score and Technique Should Be Used for Assessing Crohn's Disease Activity? J Clin Med. 2020 Jun 2;9(6):1691. doi: 10.3390/jcm9061691. PMID: 32498279; PMCID: PMC7355690.
15. Rimola J, Ordás I, Rodriguez S, García-Bosch O, Aceituno M, Llach J, Ayuso C, Ricart E, Panés J. Magnetic resonance imaging for evaluation of Crohn's disease: validation of parameters of severity and quantitative index of activity. Inflamm Bowel Dis. 2011 Aug;17(8):1759-68. doi: 10.1002/ibd.21551. Epub 2010 Nov 8. PMID: 21744431.
16. Moy MP, Sauk J, Gee MS. The Role of MR Enterography in Assessing Crohn's Disease Activity and Treatment Response. Gastroenterol Res Pract. 2016;2016:8168695. doi: 10.1155/2016/8168695. Epub 2015 Dec 27. PMID: 26819611; PMCID: PMC4706951.

17. Rozendorn N, Amitai MM, Eliakim RA, Kopylov U, Klang E. A review of magnetic resonance enterography-based indices for quantification of Crohn's disease inflammation. Therap Adv Gastroenterol. 2018 Apr 13;11:1756284818765956. doi: 10.1177/1756284818765956. PMID: 29686731; PMCID: PMC5900818.
18. Kim JS, Jang HY, Park SH, Kim KJ, Han K, Yang SK, Ye BD, Park SH, Lee JS, Kim HJ. MR Enterography Assessment of Bowel Inflammation Severity in Crohn Disease Using the MR Index of Activity Score: Modifying Roles of DWI and Effects of Contrast Phases. AJR Am J Roentgenol. 2017 May;208(5):1022-1029. doi: 10.2214/AJR.16.17324. Epub 2017 Feb 22. PMID: 28225669.
19. Ordás I, Rimola J, Alfaro I, Rodríguez S, Castro-Poceiro J, Ramírez-Morros A, Gallego M, Giner À, Barastegui R, Fernández-Clotet A, Masamunt M, Ricart E, Panés J. Development and Validation of a Simplified Magnetic Resonance Index of Activity for Crohn's Disease. Gastroenterology. 2019 Aug;157(2):432-439.e1. doi: 10.1053/j.gastro.2019.03.051. Epub 2019 Apr 3. PMID: 30953614.
20. Buisson A, Joubert A, Montoriol PF, Da Ines D, Hordonneau C, Pereira B, Garcier JM, Bommelaer G, Petitcolin V. Diffusion-weighted magnetic resonance imaging for detecting and assessing ileal inflammation in Crohn's disease. Aliment Pharmacol Ther. 2013 Mar;37(5):537-45. doi: 10.1111/apt.12201. Epub 2013 Jan 7. Erratum in: Aliment Pharmacol Ther. 2013 May;37(10):1031. Ines, D D [corrected to Da Ines, D]. PMID: 23289713.
21. Hordonneau C, Buisson A, Scanzi J, Goutorbe F, Pereira B, Borderon C, Da Ines D, Montoriol PF, Garcier JM, Boyer L, Bommelaer G, Petitcolin V. Diffusion-weighted magnetic resonance imaging in ileocolonic Crohn's disease: validation of quantitative index of activity. Am J Gastroenterol. 2014 Jan;109(1):89-98. doi: 10.1038/ajg.2013.385. Epub 2013 Nov 19. PMID: 24247212.

22. Steward MJ, Punwani S, Proctor I, Adjei-Gyamfi Y, Chatterjee F, Bloom S, Novelli M, Halligan S, Rodriguez-Justo M, Taylor SA. Non-perforating small bowel Crohn's disease assessed by MRI enterography: derivation and histopathological validation of an MR-based activity index. Eur J Radiol. 2012 Sep;81(9):2080-8. doi: 10.1016/j.ejrad.2011.07.013. Epub 2011 Sep 15. PMID: 21924572.

23. Makanyanga JC, Pendse D, Dikaios N, et al. Evaluation of Crohn's disease activity: initial validation of a magnetic resonance enterography global score (MEGS) against faecal calprotectin. Eur Radiol 2014; 24: 277–287

24. Prezzi D, Bhatnagar G, Vega R, Makanyanga J, Halligan S, Taylor SA. Monitoring Crohn's disease during anti-TNF-α therapy: validation of the magnetic resonance enterography global score (MEGS) against a combined clinical reference standard. Eur Radiol 2016;26:2107–17

25. Oussalah A, Laurent V, Bruot O, Bressenot A, Bigard MA, Régent D, Peyrin-Biroulet L. Diffusion-weighted magnetic resonance without bowel preparation for detecting colonic inflammation in inflammatory bowel disease. Gut. 2010 Aug;59(8):1056-65. doi: 10.1136/gut.2009.197665. Epub 2010 Jun 4. PMID: 20525970.

26. Thierry ML, Rousseau H, Pouillon L, Girard-Gavanier M, Baumann C, Lopez A, Danese S, Laurent V, Peyrin-Biroulet L. Accuracy of Diffusion-weighted Magnetic Resonance Imaging in Detecting Mucosal Healing and Treatment Response, and in Predicting Surgery, in Crohn's Disease. J Crohns Colitis. 2018 Nov 9;12(10):1180-1190. doi: 10.1093/ecco-jcc/jjy098. PMID: 29985999.

27. Lee JS, Kim ES, Moon W. Chronological Review of Endoscopic Indices in Inflammatory Bowel Disease. Clin Endosc. 2019 Mar;52(2):129-136. doi: 10.5946/ce.2018.042. Epub 2018 Aug 21. PMID: 30130840; PMCID: PMC6453843.

28. Mary JY, Modigliani R. Development and validation of an endoscopic index of the severity for Crohn's disease: a prospective multicentre study. Groupe d'Etudes Thérapeutiques des

Affections Inflammatoires du Tube Digestif (GETAID). Gut. 1989 Jul;30(7):983-9. doi: 10.1136/gut.30.7.983. PMID: 2668130; PMCID: PMC1434265.

29. Sipponen T, Nuutinen H, Turunen U, Färkkilä M. Endoscopic evaluation of Crohn's disease activity: comparison of the CDEIS and the SES-CD. Inflamm Bowel Dis. 2010 Dec;16(12):2131-6. doi: 10.1002/ibd.21300. PMID: 20848462.
30. Kucharski M, Karczewski J, Mańkowska-Wierzbicka D, Karmelita-Katulska K, Kaczmarek E, Iwanik K, Rzymski P, Grzymisławski M, Linke K, Dobrowolska A. Usefulness of Endoscopic Indices in Determination of Disease Activity in Patients with Crohn's Disease. Gastroenterol Res Pract. 2016;2016:7896478. doi: 10.1155/2016/7896478. Epub 2016 Feb 21. PMID: 26997952; PMCID: PMC4779516.
31. Daperno M, D'Haens G, Van Assche G, Baert F, Bulois P, Maunoury V, Sostegni R, Rocca R, Pera A, Gevers A, Mary JY, Colombel JF, Rutgeerts P. Development and validation of a new, simplified endoscopic activity score for Crohn's disease: the SES-CD. Gastrointest Endosc. 2004 Oct;60(4):505-12. doi: 10.1016/s0016-5107(04)01878-4. PMID: 15472670.
32. Sostegni R, Daperno M, Scaglione N, Lavagna A, Rocca R, Pera A. Review article: Crohn's disease: monitoring disease activity. Aliment Pharmacol Ther. 2003 Jun;17 Suppl 2:11-7. doi: 10.1046/j.1365-2036.17.s2.17.x. PMID: 12786607.
33. Rutgeerts P, Geboes K, Vantrappen G, Kerremans R, Coenegrachts JL, Coremans G. Natural history of recurrent Crohn's disease at the ileocolonic anastomosis after curative surgery. Gut. 1984 Jun;25(6):665-72. doi: 10.1136/gut.25.6.665. PMID: 6735250; PMCID: PMC1432363.
34. Rivière P, Vermeire S, Irles-Depe M, Van Assche G, Rutgeerts P, de Buck van Overstraeten A, Denost Q, Wolthuis A, D'Hoore A, Laharie D, Ferrante M. No Change in Determining Crohn's Disease Recurrence or Need for Endoscopic or Surgical Intervention With Modification of the Rutgeerts' Scoring System. Clin Gastroenterol Hepatol. 2019 Jul;17(8):1643-1645. doi: 10.1016/j.cgh.2018.09.047. Epub 2018 Oct 4. PMID: 30291910.

35. Qayyum A. Diffusion-weighted imaging in the abdomen and pelvis: concepts and applications. Radiographics. 2009 Oct;29(6):1797-810. doi: 10.1148/rg.296095521. PMID: 19959522; PMCID: PMC6939846.

36. Hagmann P, Jonasson L, Maeder P, Thiran JP, Wedeen VJ, Meuli R. Understanding diffusion MR imaging techniques: from scalar diffusion-weighted imaging to diffusion tensor imaging and beyond. Radiographics. 2006 Oct;26 Suppl 1:S205-23. doi: 10.1148/rg.26si065510. PMID: 17050517.

37. Inserra G, Conti Bellocchi MC, Foti P, Samperi L, MendolaroM, Catanzaro R. Evaluation of Crohn's disease activity by diffusion weighted magnetic resonance imaging (MRI). J Crohn's Colitis 2013;7:111.

38. A.Oto,A.Kayhan, J. T. B.Williams et al., "ActiveCrohn'sdisease in the small bowel: evaluation by diffusion weighted imaging and quantitative dynamic contrast enhanced MR imaging," Journal of Magnetic Resonance Imaging, vol. 33, no. 3, pp. 615–624, 2011.

39. S. Kiryu, K. Dodanuki, H. Takao et al., "Free-breathing diffusion-weighted imaging for the assessment of inflammatory activity in crohn's disease," Journal of Magnetic Resonance Imaging, vol. 29, no. 4, pp. 880–886, 2009.

40. A. Oto, F. Zhu, K. Kulkarni, G. S. Karczmar, J. R. Turner, D. Rubin, "Evaluation of diffusion-weighted MR imaging for detection of bowel inflammation in patients with Crohn's
disease," Academic Radiology, vol. 16, no. 5, pp. 597–603, 2009.

41. M. Freiman, J. M. Perez-Rossello, M. J. Callahan et al. Characterization of fast and slow diffusion from diffusion weighted MRI of pediatric Crohn's disease," Journal ofMagnetic Resonance Imaging, vol. 37, no. 1, pp. 156–163, 2013.

42. H. Neubauer, T. Pabst, A. Dick et al., "Small-bowel MRI in children and young adults with Crohn disease: retrospective head-to-head comparison of contrast-enhanced and diffusion weighted MRI," Pediatric Radiology, vol. 43, no. 1, pp. 103–114, 2013.

43. J. M. Ream, J. R. Dillman, J. Adler et al., “MRI diffusion weighted imaging (DWI) in pediatric small bowel Crohn disease: correlation with MRI findings of active bowel wall inflammation,” Pediatric Radiology, vol. 43, no. 9, pp. 1077–1085, 2013.
44. Wu CC, Guo WY, Chen MH, Ho DM, Hung AS, Chung HW. Direct measurement of the signal intensity of diffusion-weighted magnetic resonance imaging for preoperative grading and treatment guidance for brain gliomas. J Chin Med Assoc. 2012 Nov;75(11):581-8. doi: 10.1016/j.jcma.2012.08.019. Epub 2012 Nov 2. PMID: 23158036.
45. Chuang YH, Ou HY, Yu CY, Chen CL, Weng CC, Tsang LL, Hsu HW, Lim WX, Huang TL, Cheng YF. Diffusion-weighted imaging for identifying patients at high risk of tumor recurrence following liver transplantation. Cancer Imaging. 2019 Nov 15;19(1):74. doi: 10.1186/s40644-019-0264-y. PMID: 31730015; PMCID: PMC6858682.
46. Hollander M., Wolfe D.A., Chicken E. (2014). Nonparametric Statistical Methods, John Wiley & Sons
47. Jonckheere, A. R. (1954). A distribution-free k-sample test against ordered alternatives, Biometrika 41, 133–145
48. Le Bihan D, Breton E, Lallemand D, et al. MR imaging of intravoxel incoherent motions: application to diffusion and perfusion in neurologic disorders. Radiology 1986; 161:401–407
49. Stanescu-Siegmund N, Nimsch Y, Wunderlich AP, Wagner M, Meier R, Juchems MS, Beer M, Schmidt SA. Quantification of inflammatory activity in patients with Crohn's disease using diffusion weighted imaging (DWI) in MR enteroclysis and MR enterography. Acta Radiol. 2017 Mar;58(3):264-271. doi: 10.1177/0284185116648503. Epub 2016 Jul 12. PMID: 27178031.
50. Tielbeek JA, Ziech ML, Li Z, Lavini C, Bipat S, Bemelman WA et al. Evaluation of conventional, dynamic contrast enhanced and diffusion weighted MRI for quantitative

Crohn’s disease assessment with histopathology of surgical specimens. Eur Radiol. 2014;24(3):619-29.

51. Rosenbaum DG, Rose ML, Solomon AB, Giambrone AE, Kovanlikaya A. Longitudinal diffusion-weighted imaging changes in children with small bowel Crohn’s disease: preliminary experience. Abdom Imaging. 2015;40(5):1075-80
52. Caruso A, Angriman I, Scarpa M, D'Incà R, Mescoli C, Rudatis M, Sturniolo GC, Schifano G, Lacognata C. Diffusion-weighted magnetic resonance for assessing fibrosis in Crohn's disease. Abdom Radiol (NY). 2020 Aug;45(8):2327-2335. doi: 10.1007/s00261-019-02167-0. PMID: 31392397.
53. Cansu A, Bekircavusoglu S, Oguz S, Bulut E, Fidan S. Can diffusion weighted imaging be used as an alternative to contrast-enhanced imaging on magnetic resonance enterography for the assessment of active inflammation in Crohn disease? Medicine (Baltimore). 2020 Feb;99(8):e19202. doi: 10.1097/MD.0000000000019202. PMID: 32080107; PMCID: PMC7034637.
54. Seo N, Park SH, Kim KJ, et al. MR enterography for the evaluation of small-bowel inflammation in Crohn disease by using diffusion-weighted imaging without intravenous contrast material: a prospective noninferiority study. Radiology 2016;278:762–72
55. Rimola J, Ordás I. MR colonography in inflammatory bowel disease. Magn Reson Imaging Clin N Am 2014;22:23–33
56. Soydan L, Demir AA, Ozer S, Ozkara S. Can MR Enterography and Diffusion-Weighted Imaging Predict Disease Activity Assessed by Simple Endoscopic Score for Crohn's Disease? J Belg Soc Radiol. 2019 Jan 18;103(1):10. doi: 10.5334/jbsr.1521. PMID: 30671568; PMCID: PMC6337050.
57. Kim, KJ, Lee, Y, Park, SH, et al. Diffusion-weighted MR enterography for evaluating Crohn’s disease: How does it add diagnostically to conventional MR enterography?

Inflamm Bowel Dis. 2015; 21(1): 101–109. DOI: https://doi.org/10.1097/MIB.0000000000000222

58. Park SH. DWI at MR Enterography for Evaluating Bowel Inflammation in Crohn Disease. AJR Am J Roentgenol. 2016 Jul;207(1):40-8. doi: 10.2214/AJR.15.15862. Epub 2016 Mar 9. PMID: 26959382.
59. Pendsé DA, Makanyanga JC, Plumb AA, Bhatnagar G, Atkinson D, Rodriguez-Justo M, Halligan S, Taylor SA. Diffusion-weighted imaging for evaluating inflammatory activity in Crohn's disease: comparison with histopathology, conventional MRI activity scores, and faecal calprotectin. Abdom Radiol (NY). 2017 Jan;42(1):115-123. doi: 10.1007/s00261-016-0863-z. PMID: 27567607; PMCID: PMC5243884.
60. Klang E, Kopylov U, Eliakim R, Rozendorn N, Yablecovitch D, Lahat A, Ben-Horin S, Amitai MM. Diffusion-weighted imaging in quiescent Crohn's disease: correlation with inflammatory biomarkers and video capsule endoscopy. Clin Radiol. 2017 Sep;72(9):798.e7-798.e13. doi: 10.1016/j.crad.2017.04.006. Epub 2017 May 13. PMID: 28506799.
61. Shenoy-Bhangle AS, Nimkin K, Aranson T, Gee MS. Value of diffusion-weighted imaging when added to magnetic resonance enterographic evaluation of Crohn disease in children. Pediatr Radiol 2016; 46:34–42
62. Caruso A, D'Inca R, Scarpa M, et al. Diffusionweighted magnetic resonance for assessing ileal Crohn's disease activity. Inflamm Bowel Dis 2014; 20:1575–1583
63. Buisson A, Hordonneau C, Goutte M, Scanzi J, Goutorbe F, Klotz T, Boyer L, Pereira B, Bommelaer G. Diffusion-weighted magnetic resonance enterocolonography in predicting remission after anti-TNF induction therapy in Crohn's disease. Dig Liver Dis. 2016 Mar;48(3):260-6. doi: 10.1016/j.dld.2015.10.019. Epub 2015 Nov 22. PMID: 26699828.
64. Yu H, Feng C, Wang Z, Li J, Wang Y, Hu X, Li Z, Shen Y, Hu D. Potential of diffusion-weighted imaging in magnetic resonance enterography to identify neoplasms in the ileocecal

region: Use of ultra-high b-value diffusion-weighted imaging. Oncol Lett. 2019 Aug;18(2):1451-1457. doi: 10.3892/ol.2019.10441. Epub 2019 Jun 5. PMID: 31423210; PMCID: PMC6607208.

65. Bilgili MY. Reproductibility of apparent diffusion coefficients measurements in diffusion-weighted MRI of the abdomen with different b values. Eur J Radiol 2012;81:2066-2068
66. Braithwaite AC, Dale BM, Boll DT, Merkle EM. Short- and midterm reproducibility of apparent diffusion coefficient measurements at 3.0-T diffusion-weighted imaging of the abdomen. Radiology 2009;250:459-465
67. Kim SY, Lee SS, Byun JH, Park SH, Kim JK, Park B, et al. Malignant hepatic tumors: short-term reproducibility of apparent diffusion coefficients with breath-hold and respiratory-triggered diffusion-weighted MR imaging. Radiology 2010;255:815-823
68. Miquel ME, Scott AD, Macdougall ND, Boubertakh R, Bharwani N, Rockall AG. In vitro and in vivo repeatability of abdominal diffusion-weighted MRI. Br J Radiol 2012;85:1507-1512
69. Taouli B, Koh DM. Diffusion-weighted MR imaging of the liver. Radiology 2010;254:47-66
70. Huh J, Kim KJ, Park SH, Park SH, Yang SK, Ye BD, Park SH, Han K, Kim AY. Diffusion-Weighted MR Enterography to Monitor Bowel Inflammation after Medical Therapy in Crohn's Disease: A Prospective Longitudinal Study. Korean J Radiol. 2017 Jan-Feb;18(1):162-172. doi: 10.3348/kjr.2017.18.1.162. Epub 2017 Jan 5. PMID: 28096726; PMCID: PMC5240495.